The Power Spectrum of Run-Length-Limited Codes

AYIS GALLOPOULOS, CHRIS HEEGARD, MEMBER, IEEE, AND PAUL H. SIEGEL, MEMBER, IEEE

Abstract—**In this paper, a novel method is developed for computing formulae for the power spectra associated with run-length-limited (RLL) codes. Explicit use is made of a compact description of the run-length process associated with the RLL code. This association simplifies the general derivation of the power spectrum. The calculation of the spectra of several RLL codes popular in data storage applications is presented. Some of the closed-form expressions for the spectra of these widely used codes are new.**

I. INTRODUCTION

BINARY run-length-limited (RLL) codes, also known as (d, k) codes, are commonly used in magnetic and optical storage as well as data transmission systems. The code parameters d and k represent the minimum length and maximum length, respectively, of runs of consecutive zero symbols (0) between a pair of one symbols (1).

A two-level (or saturation) waveform, $W(t) \in \{-1, +1\}$, called the *write* (or *transmission*) signal, is used to store (or transmit) information. In practice, the write signal is synchronously generated from a binary *modulation* (or *input*) sequence $\{A_n\}$

$$W(t) = \sum_{n=-\infty}^{\infty} A_n P_T(t - nT)$$

with *clock period* T where the modulating *pulse function*

$$P_T(t) \equiv \begin{cases} 1, & \text{if } 0 \le t < T; \\ 0, & \text{otherwise.} \end{cases}$$

Note that the modulation sequence is the input to the modulator (write waveform generator) and not the raw data that is to be stored; in this respect, the input sequence is the *output* of the (d, k) encoder.

It is often useful in practice to determine the power spectrum of the write signal $W(t)$, when random data is presented to the input of the (d, k) encoder. The power spectrum of the RLL code provides a measure of bandwidth compression as well as a means of determining the average interference with embedded tracking/timing/focus servo channels due to the data signal and the signal on adjacent tracks. In this paper, a novel method is developed for computing the power spectrum of the (d, k) modulated write signal. It differs from previously published spectrum computation methods applicable to RLL coded signals, [1]–[6], in that explicit use is made of a compact description of the allowable sequence of run-lengths associated with the RLL code. This description of the code sequences, referred to as the *run-length diagram*, simplifies the derivation of a general expression for the power spectrum of run-length-limited systems, including maxentropic sequences previously considered in [7]–[8]. In addition, it provides a unified approach toward calculation of explicit formulae for the power spectra of specific RLL codes, the descriptions of which can take diverse forms, including: block codes, finite state codes, variable length codes, and look-ahead codes.

The remainder of the paper is organized as follows. Section II provides definitions and derivations of the main results. Specifically, in Section II-A, the processes associated with a run-length code are formally defined and the basic relationships between their spectra are described. In the following section, Section II-B, the general expression for the power spectrum is derived by making use of the run-length description of a run-length-limited system of sequences. It is also shown here, as a special case, that the method provides a conceptually simple derivation of the power spectra of maxentropic (d, k) codes [7], [8]. Section III provides the applications of the results. The procedure for obtaining the necessary run-length description from a (d, k) encoder is applied and the spectrum computation method is then demonstrated for several codes of practical importance in data storage applications. These examples include delay modulation or MFM [9], the IBM (2, 7) [10], the Xerox (2, 7) [11], the Jacoby (1, 7) [12], and the Adler-Hassner-Moussouris (AHM) (1, 7) [13] codes. The closed form expressions for the spectra of these widely used codes, with the exception of MFM, are new. Appendix A describes the derivation of the run-length diagram and its underlying Markov chain from a (d, k) encoder description. Appendix B provides the proofs of the main theorems relating to the general expression for the power spectrum.

II. GENERAL FORMULA FOR RLL POWER SPECTRUM

Section II-A begins with the definition of several random processes which it is convenient to associate with RLL systems of sequences. Expressions relating their power spectra are then derived. In Section II-B, the method for computing the formulae for the power spectra of these processis is outlined. As a straightforward application, a new and conceptually simple proof of the power spectrum formula for maxentropic (d, k) sequences is presented.

A. Associated Processes and Power Spectrum Relations

Formally, the binary (d, k) code sequence $\{b_n\}$ is defined as a binary sequence in which any two consecutive 1's are separated by at least d and at most k consecutive 0's. Associated with it are three discrete-time processes.

1) The Input Signal Process $[A_n]$: This is the modulation sequence described in the Introduction, with $A_n \in \{-1, +1\}$, $A_n = 1 - 2c_n$ where $c_n = c_{n-1} \oplus b_n$

2) The Output Signal Process $[X_n]$: This process is defined by the equation

$$X_n = \frac{1}{2}(A_n - A_{n-1})$$

Paper approved by the Editor for Data Communications and Modulation of the IEEE Communications Society. Manuscript received September 10, 1987; revised August 19, 1988. This work was supported in part under NSF Grant ECS-8352220. This paper was presented in part at the Workshop on Information Theory, Mathematisches Forschungsinstitute Oberwolfach, Oberwolfach, Germany, May 1986.

A. Gallopoulos and C. Heggard are with the School of Electrical Engineering, Cornell University, Ithaca, NY 14853.

P. H. Siegel is with the IBM Research Division, Almaden Research Center, K65/802, San Jose, CA 95120-6009.

IEEE Log number 8929589.

0090-6778/89/0900-0906$01.00

with $X_n \in \{0, +1, -1\}$. This process obeys $|X_n| = b_n$ with the signs of its nonzero terms alternating. It is called the output process since it can be considered as the output of a ("partial response") linear filter with the modulation sequence as input. In terms of "D-transforms,"

$$X(D) = \frac{(1-D)}{2} A(D)$$

where $(1 - D)/2$ is the *transfer function* of the filter and

$$A(D) = \sum_{n=-\infty}^{\infty} A_n D^n,$$

etc. In terms of the output signal, the (d, k) constraint means that consecutive nonzero terms are separated by at least d occurrences of 0 and at most k; if $X_n \neq 0$ then $X_{n+1} = X_{n+2} = \cdots = X_{n+d} = 0$, and $X_m \neq 0$ for some m, $n + d + 1 \leq m \leq n + k + 1$.

Due to the nature of most magnetic recording systems, the output signal $\{X_n\}$ often has special significance. In this paper, the usefulness of considering this signal relates to the method of computing the power spectrum in terms of the run-lengths; its usual significance to magnetic recording is irrelevant in this context. For example, the method works equally well for a (d, k) code used in an optical recording system where the output signal $\{X_n\}$, has no special meaning.

3) The Run-Length Process $[T_j]$: The term T_j simply counts the number of consecutive 0's together with the ending (or starting) 1 of the jth run in the code sequence $\{b_n\}$, so for a (d, k) sequence $T_j \in \{d + 1, \cdots, k + 1\}$.

If random data are presented to the input of a (d, k) encoder, then the resulting input signal, $\{A_n\}$, output signal, $\{X_n\}$, and write signal, $W(t)$, are random processes with well-defined power spectral densities. The relationships between their spectra are now derived. We introduce D-transforms and define the spectrum of a wide-sense-stationary discrete-time process $\{Y_n\}$ by

$$S_Y(D) = \sum_{j=-\infty}^{\infty} R_Y(j) D^j = \sum_{j=-\infty}^{\infty} E(Y_0 Y_j) D^j, \qquad (1)$$

where $R_Y(j)$ denotes the jth autocorrelation coefficient $E(Y_0 Y_j)$.

Since

$$X(D) = \frac{1-D}{2} A(D)$$

it follows that

$$S_X(D) = \frac{2 - (D + D^{-1})}{4} S_A(D).$$

Evaluating at $D = e^{i2\pi f}$, the spectra of the input and output processes are therefore related by the equation

$$S_X(e^{i2\pi f}) = (\sin(\pi f))^2 S_A(e^{i2\pi f}). \qquad (2a)$$

Recalling that the write signal $W(t)$ is given by

$$W(t) = \sum_{n=-\infty}^{\infty} A_n P_T(t - nT)$$

where

$$P_T(t) = \begin{cases} 1, & \text{if } 0 \leq t < T \\ 0, & \text{otherwise.} \end{cases},$$

it follows that for all $f \neq 0$

$$S_W(f) = \left(\frac{\sin(\pi f T)}{\pi f T}\right)^2 T^2 S_A(e^{i2\pi f T}) \qquad (2b)$$

and for $f = 0$,

$$S_W(0) = T^2 S_A(1).$$

These equations imply that, given the spectrum of the output process $\{X_n\}$, the spectrum of the input signal $\{A_n\}$ and the write signal $W(t)$ are determined *except* for the value at $f = 0$. The continuous portions of the spectra of $W(t)$ and $\{A_n\}$ are determined by $S_X(e^{i2\pi f})$ by taking the limit as $f \to 0$. The discrete portions of the spectra of $W(t)$ and $\{A_n\}$ have a discrete spectral line at $f = 0$ with amplitude given by $(m_W)^2$ and $(m_A)^2$, respectively, where m_W is the mean or dc value of the write process, and m_A is the mean value of the input process. Since the mean value of the output process is always zero, the means of $W(t)$ and $\{A_n\}$, which are equal, must be computed independently of the knowledge of $S_X(e^{i2\pi f})$.

In the practical codes which we consider, $\{b_n\}$, $\{A_n\}$, and $\{X_n\}$ are cyclostationary processes and therefore not wide-sense-stationary. This results from the fact that practical encoders are representable as finite-state machines with fixed input and output block lengths, where we assume that encoder inputs are independent and identically distributed.

Thus, it is not possible to define the spectrum of, say, $\{A_n\}$ as the discrete time Fourier transform of its autocorrelation function. Instead, we define another process $\{Z_n\}$ by $Z_n = A_{n+\theta}$ where θ is a discrete random variable uniformly distributed over the period r of the $\{A_n\}$ cyclostationary process. This new process can be shown to be wide-sense-stationary. We can now define $S_A(D)$ as the spectrum of $\{Z_n\}$. The spectrum of the $\{X_n\}$ process can be defined in a similar way and it can be shown that (2a) holds even for $\{A_n\}$ and $\{X_n\}$ cyclostationary processes.

Similarly, the write signal $W(t)$ represents a cyclostationary process with period $\tau = rT$. Extending the method described above to continuous time processes, we define another process $V(t)$ by $V(t) = W(t + \phi)$ where ϕ is uniformly distributed over the period τ. We define $S_W(f)$, the spectrum of $W(t)$, as the spectrum of $V(t)$.

The relationship (2b) above holds in the context of cyclostationary processes as well.

B. Calculation of the Power Spectrum of $[X_n]$

Assume we are given a finite-state machine (FSM) that generates the (d, k) code in question, assuming equiprobable data bits. More generally, one can assume a finite-state transition diagram (FSTD) that generates the valid code sequences of a run-length constrained system according to a prescribed set of transition probabilities, which in most applications maximize the entropy of the system.

By a process involving splitting and merging of states, described in the Appendix, we show that we obtain a Markov chain $\{S_n\}$ on states $\{1, 2, \cdots, L\}$ such that the run-length process $\{T_n\}$ is a function of the Markov chain $\{S_n\}$, in the sense that $\Pr(T_n = t | S_{n-1}, \cdots, S_0, T_{n-1}, \cdots, T_0) = \Pr(T_n = t | S_{n-1})$.

This run-length process is then represented by a labeled directed graph, which we call the *run-length diagram*. Each directed edge connecting state i to state j has a label t, corresponding to the length of the run completed.

Also associated with each edge is the transition probability inherited from the underlying Markov chain, $p_{ij}(t)$, which corresponds to the conditional transition probability for a run of length t from state i to state j, that is, the conditional probability of completing exactly one run of $(t - 1)$ 0's followed (or preceded) by a single 1, from state i to state j.

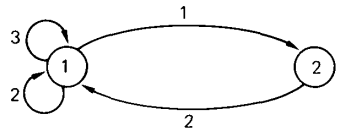

Fig. 1. Example run-length diagram.

With this description, the run-length constrained system assumes the form of a *discrete noiseless channel* [14], with variable length symbols corresponding to runs. The underlying Markov chain defines precisely the probabilities which maximize the entropy of the constrained system when viewed as an information source.

On the run-length diagram we can define a *one-step state-transition matrix* $G(D)$ with general entry $g_{ij}(D)$ given by

$$g_{ij}(D)=\sum_{t=d+1}^{k+1} p_{ij}(t)D^t.$$

For example, Fig. 1 shows a two state run-length diagram with associated transition probabilities. The corresponding one step state-transition matrix is given by

$$G(D)=\begin{pmatrix} p_{11}(2)D^2+p_{11}(3)D^3 & p_{12}(1)D \\ p_{21}(2)D^2 & 0 \end{pmatrix}.$$

Recalling the theory of Markov chains [15], it is not hard to see that the general entry $g_{ij}^n(D)$ of $[G(D)]^n$, $n \geq 0$, will be given by

$$g_{ij}^n(D)=\sum_{t=n(d+1)}^{n(k+1)} p_{ij}^n(t)D^t \tag{3}$$

where $p_{ij}^n(t)$ is the conditional probability of completing exactly n runs of total length t, from state i to state j. (Note that, for $n = 1$, $g_{ij}^n(D)$ and $p_{ij}^n(t)$ are simply called $g_{ij}(D)$ and $p_{ij}(t)$, respectively.) For notational convenience, we shall write

$$g_{ij}^n(D)=\sum_{t=1}^{\infty} p_{ij}^n(t)D^t \tag{4}$$

where $p_{ij}^n(t) = 0$ for $t \notin \{n(d+1), \cdots, n(k+1)\}$.

The following theorem gives a closed-form expression for the power spectrum in terms of $G(D)$ in the case where the sum $\Sigma_{j=-\infty}^{\infty} R_X(j)D^j$ converges on the unit circle. In general, it corresponds to the continuous component of the power spectrum. The situation which occurs when the sum does not converge and the spectrum has a nontrivial discrete component will be discussed in Example 3.

Theorem 1: Assuming the Markov chain $\{S_n\}$ is in equilibrium, the power spectrum $S_X(D)$ of the output signal process $\{X_n\}$ is given by

$$S_X(D)=p(1)\pi[(I+G(D))^{-1}+(I+G(D^{-1}))^{-1}-I]u^T \tag{5}$$

where

$$\pi=(\pi_1, \cdots, \pi_L)$$

is the vector of the stationary probabilities of states $1, \cdots, L$,

$$u=(1, 1, \cdots, 1)$$

is a vector with all L components equal to one and

$$p(1)=1-P(X_n=0)$$

is the equilibrium probability of a $+1$ or a -1 in the $\{X_n\}$ process.

Proof: The proof is given in the Appendix.

For applications of the theorem, it is useful to outline the procedure of obtaining the stationary distribution vector π and the equilibrium probability $p(1)$ of a symbol $+1$ or a symbol -1 in the $\{X_n\}$ process. Note that $G(1)$ is simply the ordinary one step transition probability matrix of the Markov chain $\{S_n\}$. Clearly π can be obtained by solving the equation

$$\pi G(1)=\pi \tag{6}$$

together with the normalizing condition

$$\sum_{i=1}^{L} \pi_i=1. \tag{7}$$

On the other hand, assuming stationarity and ergodicity of the run-length process $\{T_j\}$, $p(1)$ is simply the reciprocal of the average run-length $E(T_j)$. (See, for example, Petersen [16].) An expression for $E(T_j)$ is provided by the following theorem.

Theorem 2: The mean value of the run-length process $\{T_j\}$ is given by

$$E(T_j)=\pi G'(1)u^T$$

where $G'(1)$ is the derivative of $G(D)$ with respect to D at the point $D = 1$ and π and u are as before.

Thus,

$$p(1)=[\pi G'(1)u^T]^{-1}. \tag{8}$$

Proof: The proof is given in the Appendix.

We now discuss some applications of Theorem 1.

Example 1: Maxentropic (d, k) Constraints: As a special case, consider i.i.d. run-lengths $\{T_j\}$ generated by a trivial run-length diagram consisting of a single state. Then $G(D)$ is a polynomial and the expression for $S_X(D)$ reduces to

$$S_X(D)=p(1)[1-G(D)G(D^{-1})]/(1+G(D))(1+G(D^{-1})), \tag{9}$$

the result derived in 1942 by Foley [see, for example, 17] in another context and recently rederived by Zehavi and Wolf [8]. In the case of (d, k) codes achieving maximum entropy (known as *maxentropic codes*) [7], the run-lengths follow a truncated geometric distribution with parameter λ. Then

$$G(D)=\sum_{j=d+1}^{k+1} \lambda^{-j}D^j \tag{10}$$

where λ is the largest positive root of the equation $x^{k+1} = x^{k-d} + x^{k-d-1} + \cdots + 1$. Note that

$$\pi_1=1$$

and $p(1)$ is given by

$$p(1)=1\Big/\sum_{j=d+1}^{k+1} j\lambda^{-j}.$$

Example 2: Maxentropic (d_1, k_1) – (d_2, k_2) Constraints: Interleaved run-length-limited constraints have been proposed for use in optical storage channels where the minimum written mark length may differ from the minimum

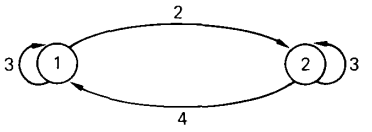

Fig. 2. Example of run-length diagram for periodic binary symbol process.

allowable spacing between marks. These sequences are characterized by parameters $(d_1, k_1) - (d_2, k_2)$ which describe the constraints on alternate run-lengths of zeros. The associated two-state maxentropic run-length process is therefore obtained by interleaving two (d, k) run-length processes with parameters (d_1, k_1) and (d_2, k_2), respectively.

In this case, we find

$$G(D)=\begin{pmatrix} 0 & (\Sigma_{j=d_1+1}^{k_1+1}\lambda^{-j}D^{-j})/\Sigma_{j=d_1+1}^{k_1+1}\lambda^{-j} \\ (\Sigma_{m=d_2+1}^{k_2+1}\lambda^{-m}D^{-m})/\Sigma_{m=d_2+1}^{k_2+1}\lambda^{-m} & 0 \end{pmatrix}$$

where λ is the largest positive root of the equation

$$\left(\sum_{j=d_1+1}^{k_1+1} x^{-j}\right)\left(\sum_{m=d_2+1}^{k_2+1} x^{-m}\right)=1.$$

Moreover, a simple calculation shows that

$$\pi=\left(\frac{1}{2},\frac{1}{2}\right)$$

and

$$p(1)=2/(ET_1+ET_2),$$

where

$$ET_1=\left(\sum_{j=d_1+1}^{k_1+1} j\lambda^{-j}\right)\Big/\left(\sum_{j=d_1+1}^{k_1+1}\lambda^{-j}\right)$$

and

$$ET_2=\left(\sum_{m=d_2+1}^{k_2+1} m\lambda^{-m}\right)\Big/\left(\sum_{m=d_2+1}^{k_2+1}\lambda^{-m}\right).$$

The input process corresponding to this stationary chain is easily seen to have mean 0. In practice, one often restricts attention to the subsystem of input sequences in which symbols $+1$ are restricted to "mark" runs and symbols -1 are restricted to "space" runs, or vice versa. The mean value of the corresponding input process in these cases will be

$$\pm\frac{E(T_1)-E(T_2)}{E(T_1)+E(T_2)}.$$

The extension to constraints obtained by interleaving n such RLL processes, $n > 2$, is straightforward.

Example 3: Discrete Spectral Components: It is important to examine the case of a periodic autocorrelation function of the transition process $\{X_n\}$. The case is subtle and deserves special attention since the sum $\Sigma_{j=-\infty}^{\infty} R_X(j)D^j$ does not converge in the usual sense on the unit circle. The effect of periodicity is illustrated by means of the following example.

Consider the run-length diagram in Fig. 2. By looking at cycles, we can easily see that the underlying binary symbol process is periodic with period 3. Also,

$$G(D)=\begin{pmatrix} (1-\alpha)D^3 & \alpha D^2 \\ \beta D^4 & (1-\beta)D^3 \end{pmatrix}$$

where α and β are the transition probabilities from state 1 to state 2 and vice versa, respectively.

The formal inverse of $I + G(D)$ is given by

$$[I+G(D)]^{-1}=\frac{1}{1+(2-\alpha-\beta)D^3+(1-\alpha-\beta)D^6}\cdot\begin{pmatrix} 1+(1-\beta)D^3 & -\alpha D^2 \\ -\beta D^4 & 1+(1-\alpha)D^3 \end{pmatrix}.$$

The stationary probability distribution is

$$\pi=\left(\frac{\beta}{\alpha+\beta},\frac{\alpha}{\alpha+\beta}\right).$$

Thus,

$$\pi[I+G(D)]^{-1}u^T=\frac{(\alpha+\beta)-\alpha\beta D^2+[\alpha(1-\alpha)+\beta(1-\beta)]D^3-\alpha\beta D^4}{(\alpha+\beta)[1+(2-\alpha-\beta)D^3+(1-\alpha-\beta)D^6]}$$

$$=\frac{(\alpha+\beta)-\alpha\beta D^2+[\alpha(1-\alpha)+\beta(1-\beta)]D^3-\alpha\beta D^4}{(\alpha+\beta)(1+D^3)[1+(1-\alpha-\beta)D^3]}$$

which, according to Theorem 1, is equal to

$$\frac{1}{p(1)}\sum_{j=0}^{\infty}R_X(j)D^j=\frac{1}{p(1)}\sum_{j=0}^{\infty}E(X_0X_j)D^j.$$

Expanding in partial fractions

$$\pi[I+G(D)]^{-1}u^T=\frac{(\alpha^2+\beta^2)+\alpha\beta D-\alpha\beta D^2}{(\alpha+\beta)^2(1+D^3)}+\frac{2\alpha\beta-\alpha\beta D+\alpha\beta(1-\alpha-\beta)D^2}{(\alpha+\beta)^2[1+(1-\alpha-\beta)D^3]}. \quad (11)$$

The expression of the right-hand side of the equation shows clearly the two components of $(1/p(1))\ \Sigma_{j+0}^{\infty} R_X(j)D^j$. The first term is the *discrete* component which is responsible for spectral lines at frequencies corresponding to the roots of the denominator, which are the cubic roots of -1. The second term is the *continuous* component. Note that the denominator of this term has no roots on the unit circle.

The discrete component simply corresponds to the D-transform of the periodic part of the autocorrelation function $R_X(j)$, $j \geq 0$. Since the sum $\Sigma_{j=0}^{\infty} R_X(j)D^j$ for periodic $R_X(j)$ does not converge for $|D| = 1$, we have to define the D-transform of the periodic parts as the limit of Cesaro sums [18] rather than regular sums. We then find, using inverse D-transforms, that the periodic part $R_X^d(j)$, $j \geq 0$ of the autocorrelation function is

$$\frac{1}{3(\alpha+\beta)^2}\left[2(\alpha^2+\beta^2+\alpha\beta)\cos\left(\frac{2\pi j}{6}\right)+(\alpha-\beta)^2\cos\left(\frac{2\pi j}{2}\right)\right].$$

Thus, the discrete part of the spectrum $S_X^d(f)$ will consist of lines of amplitude

$$\frac{\alpha^2+\beta^2+\alpha\beta}{3(\alpha+\beta)^2}$$

at frequencies $\pm 1/6$ along with lines of amplitude

$$\frac{(\alpha-\beta)^2}{6(\alpha+\beta)^2}$$

at frequencies $\pm 1/2$.

An argument involving Cesaro sums also accounts for the fact that, by substituting (11) in Theorem 1, we obtain the correct expression for the continuous component $S_X^c(D)$ of the spectrum, namely,

$$S_X^c(D) = p(1)\frac{\alpha\beta(2-\alpha-\beta)(2-(D+D^{-1}))}{(\alpha+\beta)[1+(1-\alpha-\beta)D^3][1+(1-\alpha-\beta)D^{-3}]}.$$

To finish our discussion of this example, we let $\alpha = \beta = 1/2$ (which incidentally yields the maximum value for the entropy of this Markov chain). Then

$$R_X^d(j)=\frac{1}{2}\cos\left(\frac{2\pi j}{6}\right), j\geq 0$$

and

$$S_x^c(D)=\frac{p(1)}{4}(2-(D+D^{-1})).$$

Thus, the power spectrum will consist of spectral lines of amplitude 1/4 at frequencies $f = \pm 1/6$ along with a continuous part equal to $p(1)(\sin(\pi f))^2$.

To summarize, if the underlying binary symbol process is periodic with period p, we compute $\pi[I + G(D)]^{-1}u^T = P(D)/Q(D)$ where $Q(D) = U(D)V(D)$, with $U(D)$ having all the roots on the unit circle and $V(D)$ all the roots *not* on the unit circle. We now expand into partial fractions to obtain

$$[I+G(D)]^{-1}=\frac{T(D)}{U(D)}+\frac{W(D)}{V(D)}.$$

The periodic part $R_X^d(j)$, $j \geq 0$ of the autocorrelation function can be determined from $T(D)/U(D)$ when the latter is expanded as a formal power series in the parameter D. Since $R_X^d(j)$ is known to be an even function of j, the whole of the periodic part of the autocorrelation function is known. The discrete part of the spectrum is determined by this periodic part of $R_X(j)$. The continuous part of the spectrum is obtained by applying Theorem 1.

We remark that the existence of a non-trivial discrete spectrum can be determined readily by examination of the roots of det $[I + G(D)]$ which lie on the unit circle. In order to better understand which roots can occur, we make use of the identity

$$\det[I+G(D)]=\frac{\det[I-G^2(D)]}{\det[I-G(D)]}.$$

If the underlying binary symbol process corresponding to $G(D)$ has period p, by the Perron–Frobenius theorem [19], $(1 - D^p)$ divides det $[I - G(D)]$, and all roots which lie on the unit circle are accounted for by this factor.

With respect to $G^2(D)$, there are two cases to consider.

Case 1: $G(1)$ is a matrix with period 2.

Then the binary process underlying $G^2(D)$ has period p, and the condition on $G(1)$ implies that the roots of det $[I - G^2(D)]$ which lie on the unit circle are all accounted for by a factor $(1 - D^p)^2$ which divides det $[I - G^2(D)]$. The spectral lines therefore occur at frequencies corresponding to the roots of $1 - D^p$.

Case 2: $G(1)$ is a matrix with period unequal to 2

Then the binary process underlying $G^2(D)$ will have period either p or $2p$.

If the period is p, then the roots of the numerator which lie on the unit circle are all accounted for by a factor $(1 - D^p)$ which divides det $[I - G^2(D)]$. These roots are cancelled by the roots of the denominator, implying that the discrete spectrum is trivial (no spectral lines).

If the period is $2p$, then the roots of the numerator which lie on the unit circle are all accounted for by a factor $(1 - D^{2p})$ which divides det $[I - G^2(D)]$. The roots of the denominator are cancelled, leaving the roots of $(1 + D^p)$. The spectral lines therefore occur at frequencies corresponding to the roots of $1 + D^p$.

TABLE I
ENCODING TABLE FOR MFM

State / Data	a	b
0	00/b	10/b
1	01/a	01/a

III. Applications

In this section, we use the preceding theorems to derive explicit formulae for the power spectra of several of the most widely used run-length-limited codes: the rate 1/2 (1, 3) code known as MFM, delay modulation, or Miller code; the rate 1/2 (2, 7) codes introduced by IBM and Xerox; and the rate 2/3 (1, 7) codes derived by Jacoby and Adler-Hassner-Moussouris. The formula for the power spectrum of MFM has been previously published [9], and we present it here simply to illustrate the method. The formulae for the (2, 7) and (1, 7) codes are new. In all of the described codes, data bits are assumed to be generated by an equiprobable binary source.

A. MFM Code

Modified frequency modulation (MFM) is a simple example of a rate 1/2 (1, 3) code. The coding rules are easily described in words: a data bit "1" generates the codeword "01," and a data bit "0" generates a codeword "10" if preceded by a data bit "0," or a codeword "00" if preceded by a data bit "1."

These rules are easily translated into a two-state FSM representation of the code, as shown in Table I.

The state "*a*" represents the condition that the previous data bit was a "1," while the state "*b*" indicates that the previous data bit was a "0." A FSTD representation of the MFM code sequences is obtained from the FSM diagram by restricting edge labels to show codewords only, as seen in Fig. 3(a). The run-length diagram for MFM is easily obtained from the FSTD by the method described in the appendix, as shown in Fig. 3(b) and (c).

From the run-length diagram and the associated Markov chain, the matrix $G(D)$ can be readily obtained. Specifically, we find

$$G(D)=\begin{pmatrix}\frac{1}{2}D^2+\frac{1}{4}D^4 & \frac{1}{4}D^3\\ \frac{1}{2}D^3 & \frac{1}{2}D^2\end{pmatrix}$$

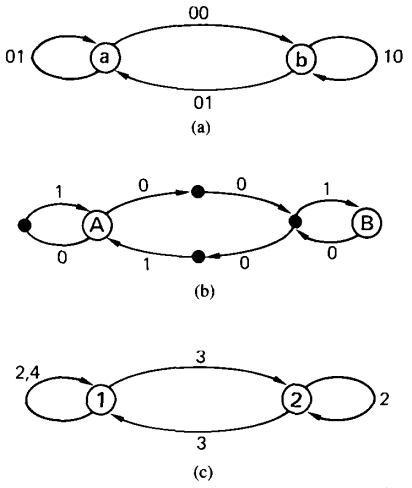

Fig. 3. (a) FSTD for MFM code. (b) Modified FSTD with inserted states. (c) Run-length diagram for MFM code.

To obtain π, we simply solve the system of equations

$$(\pi_1, \pi_2)G(1) = (\pi_1, \pi_2)$$
$$\pi_1 + \pi_2 = 1.$$

Solving, we get

$$\pi = (\pi_1, \pi_2) = \left(\frac{2}{3}, \frac{1}{3}\right).$$

Finally, as explained in Theorem 2, $p(1) = 1/E(T_n)$ where

$$E(T_n)\pi G'(1)u^T = \frac{8}{3}.$$

Therefore,

$$p(1) = \frac{3}{8}.$$

Evaluating (5), we arrive at the power spectrum for the output signal process associated with MFM

$$S_X(D) = \frac{1}{8}\left[\frac{10 - 6(D + D^{-1}) + 4(D^2 + D^{-2}) - 4(D^3 + D^{-3}) + (D^4 + D^{-4})}{9 + 6(D^2 + D^{-2}) + 2(D^4 + D^{-4})}\right].$$

The power spectrum for the input process associated with MFM is then computed to be

$$S_A(D) = \frac{1}{2}\left[\frac{6 + (D + D^{-1}) + 2(D^2 + D^{-2}) - (D^3 + D^{-3})}{9 + 6(D^2 + D^{-2}) + 2(D^4 + D^{-4})}\right].$$

It is not difficult to check, using the conditions described at the end of Section II-B, that the discrete spectrum is trivial (no spectral lines).

The write signal power spectrum of the MFM code at frequency f, $S_W(f)$, is compared to that of the maxentropic (1, 3) code in Fig. 4.

TABLE II
IBM AND XEROX (2, 7) CODES

Data	Code	Data	Code
10	0100	1	X0
11	1000	01	0001
000	000100	001	000010
010	100100	000	001001
011	001000		
0010	00100100		
0011	00001000		
	IBM code		Xerox code

$X = 1$, *if possible*; *else* 0

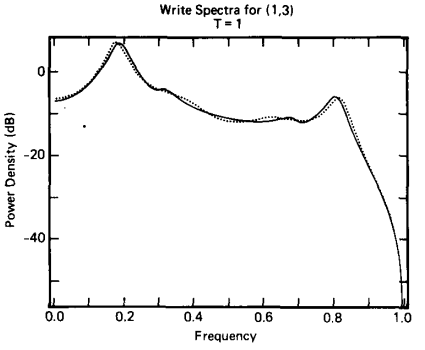

Fig. 4. (1, 3) write signal spectra: maxentropic (dashed) and implemented (solid).

B. (2, 7) Codes

Two popular rate 1/2 (2, 7) codes are the IBM [10] and Xerox [11] codes. The encoding tables for these variable length codes are shown in Table II.

The derivation of the run-length diagram for the IBM code is shown in Fig. 5. The initial FSTD is a one-state representation of the variable-length block code, Fig. 5(a). After inserting additional states in order to ensure one code symbol per edge, there are 9 states denoted $A, B, \cdots, I$ for which all incoming edges are labled with "1." The remaining states have all incoming edges labeled with "0." Consequently, no state splitting is required, Fig. 5(b). It can be seen easily that in the final run-length diagram, state merging will reduce the number of states to only 3. Specifically, states B, F, and I have identical outgoing edge structure and are combined to form state 1. Likewise, D and G combine to form state 2, and A, C, E, H merge into state 3. The result is a three-state run-length diagram. Fig. 5(c).

It is a welcome coincidence that the Xerox code has the same run-length diagram as the IBM code. A simple proof of this is shown in Fig. 6. The Xerox code is equivalent to a two-state variable-length code, in which state "a" corresponds to the condition that the past code sequence ends in 2 or more symbols "0" (implying the next $X = 1$ in Table II), and state "b" represents less than 2 (implying the next $X = 0$). The corresponding FSTD is shown in Fig. 6(a). Insertion of additional states along the loops at state b, Fig. 6(b), followed by merging of states with a single incoming edge from state b with label "00," Fig. 6(c), reproduces the one-state variable-length block code representation of the IBM code, Fig. 6(d). The two codes therefore generate the same set of code

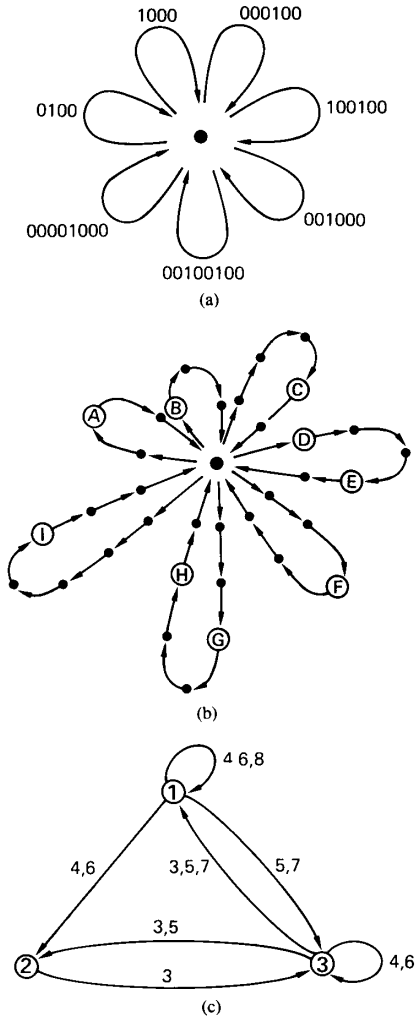

Fig. 5. (a) Variable length block code diagram for IBM (2, 7) code. (b) Diagram with inserted states for IBM (2, 7) code. (c) Reduced run-length diagram for IBM (2, 7) code.

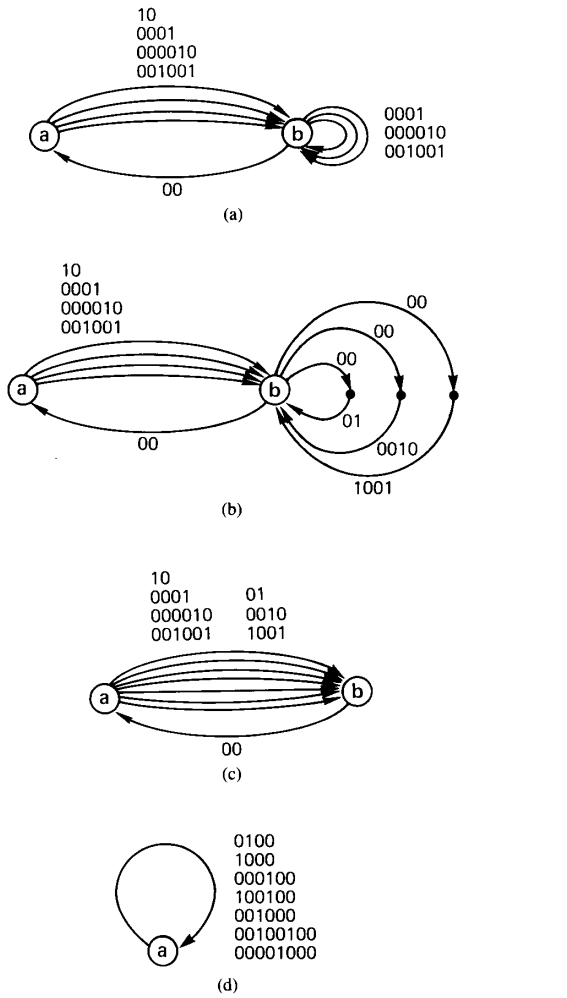

Fig. 6. (a) Finite-state variable length diagram for Xerox (2, 7) code. (b) Diagram with inserted states for Xerox (2, 7) code. (c) After merging of states with "00" incoming edge label. (d) Reduction of Xerox (2, 7) code to IBM (2, 7) code.

sequences, but the assignment of data sequences to code sequences is different.

For the (2, 7) code run-length diagram, the one step state-transition matrix can be found to be

$$G(D)=\begin{pmatrix} \frac{1}{4}D^4+\frac{1}{8}D^6+\frac{1}{16}D^8 & \frac{1}{8}D^4+\frac{1}{16}D^6 & \frac{1}{4}D^5+\frac{1}{8}D^7 \\ 0 & 0 & D^3 \\ \frac{1}{4}D^3+\frac{1}{8}D^5+\frac{1}{16}D^7 & \frac{1}{8}D^3+\frac{1}{16}D^5 & \frac{1}{4}D^4+\frac{1}{8}D^6 \end{pmatrix}.$$

Using (6) and (7), we can solve for the stationary probability vector π to get

$$\pi=(\pi_1,\ \pi_2,\ \pi_3)=\left(\frac{7}{19},\ \frac{3}{19},\ \frac{9}{19}\right).$$

Using (8), we get

$$p(1)=\frac{19}{84}.$$

The power spectrum of the input signal process associated with these (2, 7) codes is found to be

$$S_A(D)=\frac{1}{21}\frac{P(D)}{Q(D)}$$

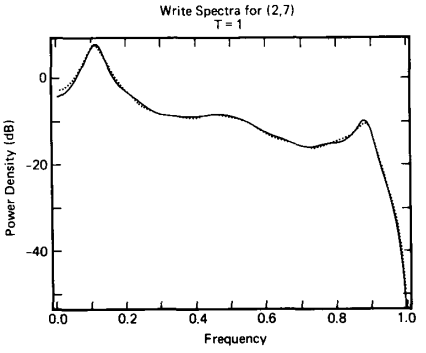

Fig. 7. (2, 7) write signal spectra: maxentropic (dashed) and implemented (solid).

TABLE III
JACOBY (1, 7) ENCODING TABLES

Data	Code	Data	Code
00	101	00.00	101.000
01	100	00.01	100.000
10	001	10.00	001.000
11	010	10.01	010.000
Basic Table		Violation Substitution Table	

where

$$P(D) = 1956 + 732(D + D^{-1}) + 212(D^2 + D^{-2}) - 381(D^3 + D^{-3}) + 27(D^4 + D^{-4}) - 204(D^5 + D^{-5}) + 4(D^6 + D^{-6}) - 80(D^7 + D^{-7}) + 16(D^8 + D^{-8}) + 24(D^9 + D^{-9}) + 24(D^{10} + D^{-10})$$

and

$$Q(D) = 162 + 8(D^2 + D^{-2}) + 64(D^4 + D^{-4}) + 16(D^6 + D^{-6}).$$

It is again not difficult to check, using the conditions described at the end of Section II-B, that the discrete spectrum is trivial (no spectral lines).

The write signal power spectrum of the IBM/Xerox codes at frequency f, $S_W(f)$, is compared to that of the maxentropic (2, 7) code in Fig. 7.

C. (1, 7) Codes

Two rate 2/3 (1, 7) codes that appear in disk storage products are the Jacoby code [12] and the AHM (IBM) code [13]. The Jacoby code is a "look-ahead" code, and is defined by the encoding rules shown in Table III. The basic encoding table in used when the resulting codeword will not cause a violation of the $d = 1$ constraint. Certain juxtapositions of data words, however, would lead to violations in the code sequence. In these cases, one changes the assignment of the current and preceding codewords in accordance with the violation substitution table.

The AHM code is described by the finite-state-machine shown in Table IV, with states designated by the letters "*a*," "*b*," "*c*," "*d*," and "*v*."

The FSTD for the AHM (1, 7) code is shown in Fig. 8(a). The run-length diagram and associated Markov chain are derived using the method of the Appendix. The three state run-length diagram is shown in Fig. 8(b).

The run-length diagram for the Jacoby code turns out to be identical to that of the AHM code. To see this easily, define a

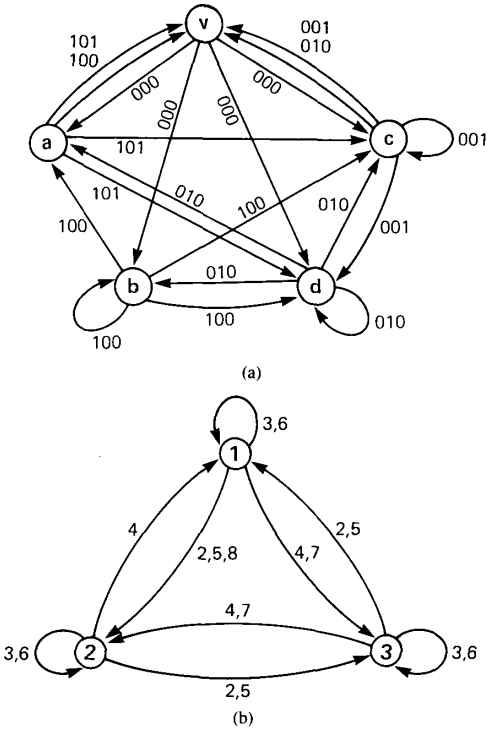

Fig. 8. (a) Finite-state transition diagram for AHM (1, 7) code. (b) Reduced run-length diagram for AHM (1, 7) code.

TABLE IV
AHM (1, 7) ENCODING TABLES

Data \ State	a	b	c	d	v
00	101/d	100/d	001/d	010/d	000/d
01	101/c	100/c	001/c	010/c	000/c
10	101/v	100/b	001/v	010/b	000/b
11	100/v	100/a	010/v	010/a	000/a

TABLE V
FSM DESCRIPTION OF JACOBY (1, 7) CODE

Data \ State	a	b	c	d	v
11	101/d	100/d	001/d	010/d	000/d
10	101/c	100/c	001/c	010/c	000/c
01	100/v	100/b	010/v	010/b	000/b
00	101/v	100/a	001/v	010/a	000/a

FSM with states "*a*," "*b*," "*c*," "*d*" corresponding to the condition that the previous data block was "00," "01," "10," or "11," respectively (and caused no violation), and state "*v*" corresponding to the condition that a violation has occurred. Edge labels are obtained from the look-ahead code table by delaying the output codewords by one block. This delay accounts for the dependence of the output codeword on one look-ahead data block. The resulting FSM table is shown in Table V.

Restricting to codeword labels in the diagrams corresponding to Tables IV and V produces FTSD's which are identical.

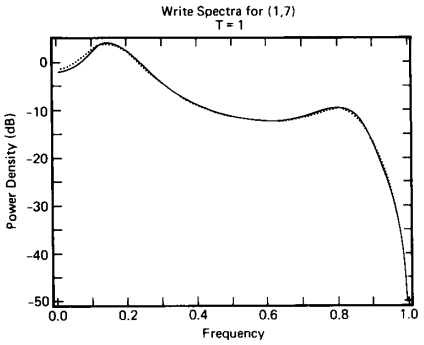

Fig. 9. (1, 7) write signal spectra: maxentropic (dashed) and implemented (solid).

As in the case of the (2, 7) codes, the two independently discovered (1, 7) codes generate identical sets of code sequences, but use different assignments of data sequences to code sequences.

Remark: T. Howell [20] has observed that the set of code sequences of the (1, 7) code is invariant under time reversal. This fact can be proved readily from Fig. 8(b) by noting that the run-length diagram is invariant under reversal of the arrows on the directed edges.

The one step state-transition matrix for the (1, 7) code is given by

$$G(D)=\begin{pmatrix} \frac{1}{4}D^3+\frac{1}{16}D^6 & \frac{3}{8}D^2+\frac{3}{32}D^5+\frac{3}{128}D^8 & \frac{5}{32}D^4+\frac{5}{128}D^7 \\ \frac{1}{6}D^4 & \frac{1}{4}D^3+\frac{1}{16}D^6 & \frac{5}{12}D^2+\frac{5}{48}D^5 \\ \frac{2}{5}D^2+\frac{1}{10}D^5 & \frac{3}{20}D^4+\frac{3}{80}D^7 & \frac{1}{4}D^3+\frac{1}{16}D^6 \end{pmatrix}$$

Using (6), (7), and (8), we obtain

$$\pi=(\pi_1,\ \pi_2,\ \pi_3)=\left(\frac{24}{73},\ \frac{24}{73},\ \frac{25}{73}\right).$$

and

$$p(1)=\frac{73}{240}.$$

The power spectrum of the input signal process associated with these (1, 7) codes is given by

$$S_A(D)=\frac{1}{15}\frac{U(D)}{V(D)}$$

where

$$\begin{aligned} U(D)=&\,15681+4591(D+D^{-1})-48(D^2+D^{-2}) \\ &+5665(D^3+D^{-3})+1498(D^4+D^{-4}) \\ &-889(D^5+D^{-5})+892(D^6+D^{-6}) \\ &+408(D^7+D^{-7})-100(D^8+D^{-8}) \end{aligned}$$

and

$$\begin{aligned} V(D)=&\,1665+968(D^3+D^{-3}) \\ &+280(D^6+D^{-6})+32(D^9+D^{-9}). \end{aligned}$$

Once again, it is not difficult to check, using the conditions described at the end of Section II-B, that the discrete spectrum is trivial (no spectral lines).

The write signal power spectrum of the Jacoby/AHM codes at frequency f, $S_W(f)$, is compared to that of the maxentropic (1, 7) code in Fig. 9.

Finally, in Fig. 10, the write signal spectra of the MFM, (2, 7) and (1, 7) codes are compared at fixed data rate.

D. Spectrum at Zero Frequency

It is often of value to have a measure of the spectrum at zero frequency of the channel input signal process [7]. The implemented codes discussed in this section all have vanishing discrete spectral lines at zero frequency, so, using the formulae for code spectral densities that we have derived, it is now an easy matter to find the value of $S_A(1)$ for MFM and the implemented (2, 7) and (1, 7) codes. The results are given in Table VI. The values for the corresponding maxentropic run-length constrained systems, discussed in Example 1, are included for comparison purposes.

Appendix A
Derivation of Run-Length Markov Chain

The run-length diagram is derived by a sequence of transformations of the finite-state transition diagram (FSTD) of the binary constrained system. First, states are inserted along edges of the initial FSTD as required to ensure that each edge generates a single symbol, as shown schematically in Fig. 11.

The next objective is to represent the system by a FSTD in which each state has all of its incoming edges labeled identically. This is accomplished by performing input splitting operations on the states of the diagram, as illustrated in Fig. 12. Fig. 12 shows a local transformation at state s of the FSTD G which we refer to as an input splitting at state s. The result is a FSTD G' with the property that each state derived from s in the splitting has all of its incoming edges labeled identically with either "0" or "1." Note that G' generates the same system of constrained sequences as G.

The input splitting operation is repeated at all states as required to produce a FSTD H with the desired property. The

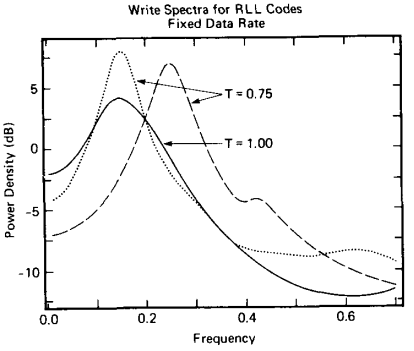

Fig. 10. Write signal spectra of MFM, IBM (2, 7), and IBM (1, 7) codes at fixed data rate.

TABLE VI
SPECTRUM AT ZERO FREQUENCY FOR MAXENTROPIC AND IMPLEMENTED CODES

Constraint	Maxentropic	Implemented
(1,3)	$\approx .23$	$\frac{1}{5} = .20$
(2,7)	$\approx .52$	$\frac{3}{8} \approx .38$
(1,7)	$\approx .73$	$\frac{47}{75} \approx .63$

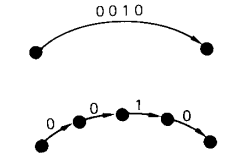

Fig. 11. Insertion of states along edge.

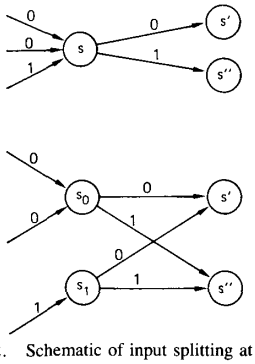

Fig. 12. Schematic of input splitting at state s.

states in H which have all incoming edges labeled with the binary symbol "1," denoted $\{s_1, \cdots, s_L\}$, correspond to the states in the run-length diagram, denoted $\{\sigma_1, \cdots, \sigma_L\}$. A run of length t is a sequence of $t-1$ symbols "0" followed by a symbol "1." There is an edge with label t from σ_i to σ_j in the run-length diagram if and only if there is a path of length t in H from s_i to s_j which generates a run of length t.

The run-length diagram can sometimes be simplified by transformations called input merging and output merging. Fig. 13 shows the local transformation corresponding to the input merging of states s and s', in which the two states are merged into a single state u, provided that they have identical outgoing edge structure; that is, the set of "next states" and corresponding edge labels is identical for both states. The resulting state u has this outgoing edge structure, and its incoming edges

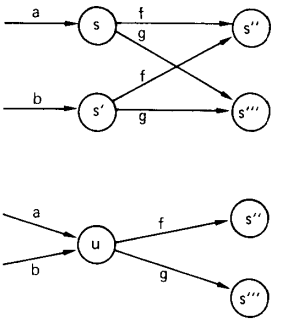

Fig. 13. Schematic of input merging.

are obtained by merging the set of edges incoming to s and s'. A depiction of an output merging transformation, which has a completely analogous description, is obtained by reversing the direction of all edges in Fig. 13, as shown in Fig. 14.

Finally, we remark that these merging operations based on the run-length diagram structure will preserve the measure of maximum entropy on corresponding system of sequences. All of the examples considered in the applications (Section III) use this maxentropic measure.

If a different measure is used, however, the input (respectively, output) merging operations can be carried out only if they respect the conditional measure on sequences emanating from (respectively, terminating at) the two states.

APPENDIX B
PROOFS OF THEOREMS

Proof of Theorem 1

Define

$$\Phi_l(D) = \sum_{j=1}^{\infty} D^j \cdot P[\text{Length of } l \text{ consecutive } T_i \text{ is } j/\text{run started}].$$

This represents a generating function for probabilities of sequences produced by l consecutive runs, where the coefficient of D^j corresponds to the probability associated with all sequences of l runs of total length j. It follows that

$$\sum_{l=0,2,4,\cdots} \Phi_l(D) - \sum_{l=1,3,\cdots} \Phi_l(D)$$

$$= 1 + \sum_{j=1}^{\infty} D^j \cdot \{P[\text{Length of an even number of consecutive } T_i \text{ is } j/\text{run started}] - P[\text{Length of an odd number of consecutive } T_i \text{ is } j/\text{run started}]\}$$

$$= 1 + \sum_{j=1}^{\infty} D^j \cdot \{P[X_j = X_0 / |X_0| = 1] - P[X_j = -X_0 / |X_0| = 1]\}$$

$$= 1 + \sum_{j=1}^{\infty} E[X_0 X_j / |X_0| = 1] \cdot D^j.$$

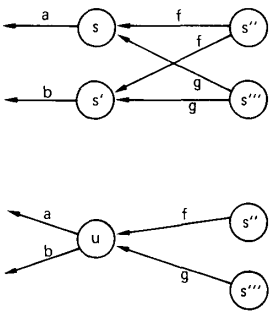

Fig. 14. Schematic of output merging.

Referring to (1), we can express the power spectrum as

$$S_X(D)=p(1)\cdot\left\{\sum_{l\,\text{even}}[\Phi_l(D)+\Phi_l(D^{-1})]-\sum_{l\,\text{odd}}[\Phi_l(D)+\Phi_l(D^{-1})]-1\right\}. \quad \text{(B1)}$$

For $\{T_i\}$ i.i.d.,

$$\Phi_l(D)=[\phi(D)]^l$$

where

$$\phi(D)=\sum_i P(T_i)D^i.$$

The power series identity

$$\frac{1}{1-x^2}=\sum_{l=0}^{\infty}x^{2l}$$

can now be applied to simplify (B1). Specifically,

$$S_X(D)=p(1)\cdot\left(\sum_{l=0,2,\cdots}([\phi(D)]^l+[\phi(D^{-1})]^l)-\sum_{l=1,3,\cdots}([\phi(D)]^l+[\phi(D^{-1})]^l)-1\right)$$

$$=p(1)\cdot\left(\frac{1}{1-[\phi(D)]^2}+\frac{1}{1-[\phi(D^{-1})]^2}-\frac{\phi(D))}{1-[\phi(D)]^2}-\frac{\phi(D^{-1})}{1-[\phi(D^{-1})]^2}-1\right)$$

$$=p(1)\cdot\left(\frac{(1-\phi(D))}{1-[\phi(D)]^2}+\frac{(1-\phi(D^{-1}))}{1-[\phi(D^{-1})]^2}-1\right)$$

$$=p(1)\cdot\frac{1-\phi(D)\cdot\phi(D^{-1})}{(1+\phi(D))\cdot(1+\phi(D^{-1}))}.$$

This recovers the result of Example 1.

More generally, for $\{T_i\}$ generated by a run-length diagram described by one-step transition matrix $G(D)$

$$\Phi_l(D)=\pi[G(D)]^l u^T.$$

Thus, we obtain

$$S_X(D)=p(1)\pi([I-(G(D))^2]^{-1}-G(D)\cdot[I-(G(D))^2]^{-1}+[I-(G(D^{-1}))^2]^{-1}-G(D^{-1})\cdot[I-(G(D^{-1}))^2]^{-1}-I)u^T$$

$$=p(1)\cdot\pi([I+G(D)]^{-1}+[I+G(D^{-1})]^{-1}-I)u^T.$$

This proves Theorem 1.

Proof of Theorem 2

The general entry $g_{ij}'(1)$ of $G'(1)$ is

$$g_{ij}'(1)=\sum_{t=d+1}^{k+1}tp_{ij}(t).$$

Therefore,

$$\pi G'(1)u^T=\sum_{i=1}^{L}\sum_{j=1}^{L}\sum_{t=d+1}^{k+1}t\pi_i p_{ij}(t)$$

$$=\sum_{t=d+1}^{k+1}tP(\text{run has length } t\,|\,\text{run started})$$

$$=E(T_n).$$

References

[1] B. Bosik, "The spectra density of a coded digital signal," *Bell Syst. Tech. J.*, vol. 51, no. 4, pp. 921–933, Apr. 1972.

[2] G. Cariolaro and G. Tronca, "Spectral of block coded digital signal," *IEEE Trans. Commun.*, vol. COM-22, pp. 1555–1564, Oct. 1974.

[3] D. Lindholm, "Power spectra of channel codes for digital magnetic recording," *IEEE Trans. Magn*, vol. MAG-14, pp. 321–323, Sept. 1978.

[4] P. Galko and S. Pasupathy, "The mean power spectral density of Markov chain driven signals," *IEEE Trans. Inform. Theory*, vol. IT-27, pp. 746–754, Nov. 1981.

[5] G. Cariolaro, G. Pierobon, and S. Pupolin, "Spectral analysis of variable-length coded digital signals," *IEEE Trans. Inform. Theory*, vol. IT-28, pp. 473–481, May 1982.

[6] G. Bilardi, R. Padovani, and G. Pierobon, "Spectral analysis of functions of Markov chains with applications," *IEEE Trans. Commun.*, vol. COM-31, pp. 853–861, July 1983.

[7] K. A. Schouhamer Immink, "Some statistical properties of maxentropic runlength-limited sequences," *Phil. J. Res.*, vol. 38, pp. 138–149, 1983.

[8] E. Zehavi and J. K. Wolf, "On run-length codes," *IEEE Trans. Inform. Theory*, vol. 34, pp. 45–54, Jan. 1988.

[9] M. Hecht and A. Guida, "Delay modulation," *Proc. IEEE*, vol. 57, pp. 1314–1316, July 1969.

[10] T. Howell, "Analysis of correctable errors in the IBM 3380 disk file," *IBM J. Research Development*, vol. 28, no. 2, pp. 206–211, Mar. 1984.

[11] K. Norris, *Xerox Discl. J.*, vol. 5, no. 6, pp. 647–648, Nov./Dec. 1980.

[12] G. Jacoby, M. Cohn, and A. Bates, III, U.S. Pat. 4 337 458, 1982.

[13] R. Adler, M. Hassner, and J. Moussouris, U.S. Pat. 4 413 251, 1982.

[14] C. Shannon and W. Weaver, *The Mathematical Theory of Communication*. Univ. Illinois Press, 1963.

[15] S. Karlin and H. Taylor, *A First Course in Stochastic Processes*. New York: Academic, 1975, pp. 58–59 and pp. 84–85.

[16] K. Petersen, *Ergodic Theory*. Cambridge University Press, 1983, p. 46.

[17] J. L. Lawson and G. E. Uhlenbeck, *Threshold Signals*. Boston Technical Publisher Inc., 1964.

[18] I. I. Hirschman, Jr., *Infinite Series*. Holt, Rinehart, and Winston, 1962.

[19] E. Seneta, *Non-negative Matrices and Markov Chains*. New York: Springer-Verlag, 1981.

[20] T. Howell, "Statistical properties of selected recording codes," *IBM Res. Rep.*, Aug. 1987.

Ayis Gallopoulos was born in Athens, Greece, on July 26, 1959. He received the B.A. degree in electrical sciences from the University of Cambridge, Cambridge, England, in 1981 and the M.S. degree in electrical engineering from Cornell University, Ithaca, NY, in 1984. He is currently enrolled in the Ph.D. program in electrical engineering at Cornell University.

★

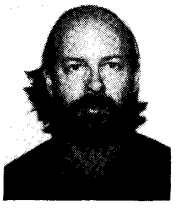

Chris Heegard (S'75–M'81) was born on October 4, 1953 in Pasadena, CA. He earned his higher education at the University of Massachusetts, Amherst, where he received the B.S. (1975) and M.S. (1976) degrees in electrical and computer engineering, and at Stanford University where he received the Ph.D. (1981) degree in electrical engineering.

For two years, 1976–1978, he was an Engineer at Linkabit Corporation in San Diego, CA. While there, he participated in the development of a digital, packet satellite modem as well as several sequential decoders. Since 1981, he has been on the faculty of the School of Electrical Engineering at Cornell University, Ithaca, NY, where he is currently an Associate Professor. During the 1987–1988 academic year he was a visitor at the IBM Almaden Research Center, San Jose, CA; during the Spring of 1988 he was also a visiting Associate at the California Institute of Technology in Pasadena, CA. He is an active participant of the technical consulting community. His research interests are in the areas of communications, information and coding theory and in the area of digital signal processing. He enjoys the application of these theories to communications and computer systems. In particular his interests are in the areas of digital recording (magnetic and optical), reliable random access memories, local area networks, data compression and digital audio.

Dr. Heegard is an active member of the IEEE publishing papers in the TRANSACTIONS OF INFORMATION THEORY, COMMUNICATIONS, and COMPUTERS. As a member of the Information Theory Group, he has participated in the organization of several meetings, was the Group's secretary for two years (1983–1985) and was elected to and actively served on the Board of Governors (1985–1988). He is currently organizing the 1989 Information Theory Workshop to be held at Cornell University, Ithaca, NY, June 26–29.

★

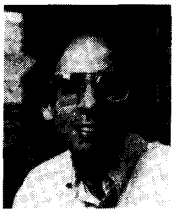

Paul H. Siegel (M'82) was born in Berkeley, CA, in 1953. He received the B.S. degree in mathematics in 1975 and the Ph.D. degree in mathematics in 1979, both from the Massachusetts Institute of Technology. He held a Chaim Weizmann fellowship during a year of postdoctoral study at the Courant Institute, New York University.

He joined the Research Staff at IBM in 1980. He is currently Manager of the Signal Processing and Coding project at the IBM Almaden Research Center in San Jose, CA. His primary research interest is the mathematical foundations of signal processing and coding, especially as applicable to digital data storage channels. He has taught courses in information and coding theory at the University of California at Santa Cruz and Santa Clara University. He holds several patents in the area of coding and detection.

Dr. Siegel was elected to Phi Beta Kappa in 1974, and is a member of the IEEE Magnetics Society, the IEEE Communications Society, the IEEE Information Theory Group, and the American Mathematical Society.